FlexTouch: Enabling Large-Scale Interaction Sensing beyond Touchscreens using Flexible and Conductive Materials

YUNTAO WANG and JIANYU ZHOU, Tsinghua University, CHINA and University of Washington, USA
HANCHUAN LI, Microsoft, USA
TENGXIANG ZHANG, Tsinghua University, CHINA and Chinese Academy of Sciences, CHINA
MINXUAN GAO, ZHUOLIN CHENG, and CHUN YU, Tsinghua University, CHINA
SHWETAK PATEL, University of Washington, USA
YUANCHUN SHI*, Tsinghua University, CHINA

In this paper, we present *FlexTouch*, a technique that enables large-scale interaction sensing beyond the spatial constraints of capacitive touchscreens using passive low-cost conductive materials. This is achieved by customizing 2D circuit-like patterns with an array of conductive strips that can be easily attached to the sensing nodes on the edge of the touchscreen. *FlexTouch* requires no hardware modification, and is compatible with various conductive materials (copper foil tape, silver nanoparticle ink, ITO frames, and carbon paint), as well as fabrication methods (cutting, coating, and ink-jet printing). Through a series of studies and illustrative examples, we demonstrate that *FlexTouch* can support long-range touch sensing for up to 4 meters and everyday object presence detection for up to 2 meters. Finally, we show the versatility and feasibility of *FlexTouch* through applications such as body posture recognition, human-object interaction as well as enhanced fitness training experiences.

CCS Concepts: • **Human-centered computing → Ubiquitous and mobile computing**; **Ubiquitous and mobile computing systems and tools**; **Human computer interaction (HCI)**; *Interaction techniques*;

Additional Key Words and Phrases: Capacitive sensing; touch interface; fabrication; large-scale interaction; posture detection.

ACM Reference Format:
Yuntao Wang, Jianyu Zhou, Hanchuan Li, Tengxiang Zhang, Minxuan Gao, Zhuolin Cheng, Chun Yu, Shwetak Patel, and Yuanchun Shi. 2019. *FlexTouch*: Enabling Large-Scale Interaction Sensing beyond Touchscreens using Flexible and Conductive Materials. *Proc. ACM Interact. Mob. Wearable Ubiquitous Technol.* 3, 3, Article 109 (January 2019), 20 pages. https://doi.org/10.1145/3351267

1 INTRODUCTION

Capacitive touchscreens are one of the most profound interaction interfaces on modern devices, providing seamless, intuitive interaction between users and digital media. However, the interface is limited to the area

*This is the corresponding author.

Authors' addresses: Yuntao Wang, yuntaowang@tsinghua.edu.cn; Jianyu Zhou, zjythu@163.com; Minxuan Gao, thss15_gaomx@163.com; Zhuolin Cheng; Chun Yu, chunyu@tsinghua.edu.cn; Yuanchun Shi, shiyc@tsinghua.edu.cn: Department of Computer Science and Technology; Key Laboratory of Pervasive Computing, Ministry of Education; Global Innovation Exchange Institute (GIX); Tsinghua University, 30 Shuangqing Rd, Beijing, 100084, CHINA. Tengxiang Zhang, Institute of Computing Technology, Chinese Academy of Sciences, No.6 Kexueyuan South Road, Zhongguancun, Haidian District, Beijing, 100190, CHINA. Hanchuan Li, hanchuan.li@microsoft.com, Microsoft, One Microsoft Way, Redmond, WA, 98052, USA. Shwetak Patel, shwetak@cs.washington.edu, University of Washington, Seattle, WA, 98105, USA.

2474-9567/2019/1-ART109 $15.00
https://doi.org/10.1145/3351267

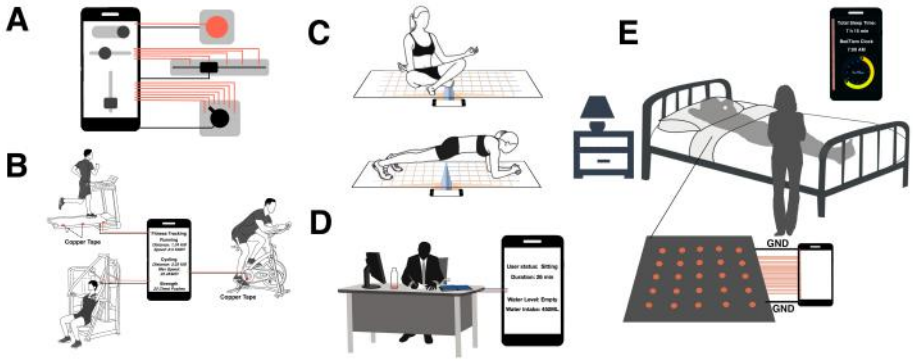

Fig. 1. *FlexTouch* supports various large-scale applications with different configurations. A: Discrete and 1-dimension touch widgets sensing long-range touch events. B: Fitness tracking using designs in A for the count of repetitions, distance and speed measurement on a treadmill, cycling and chest exercise machine. C: Body posture detection on the yoga mat with a built-in capacitive sensing matrix in an X-Y layout. D: Smart desk application for object presence and user's state detection. E. Smart mattress for sleep monitoring with a one-on-one mapping node matrix from the touchscreen.

where touch sensors are embedded, constraining natural user interactions to the surfaces of these smart devices. Scaling touchscreens to large surfaces and everyday objects is expensive and challenging, which limits its wider adoption in the Internet of Things applications.

Researchers have explored enabling touch interfaces on everyday surfaces or objects [15, 18, 19, 22, 23, 30, 33] with various sensing techniques. However, these prior work require dedicated sensing platforms such as Arduino to power touch interfaces and to enable wireless communication with digital devices. These requirements prevent end-users from easily fabricating customizable touch interfaces. As an alternative, researchers have proposed extending the capacitive sensing capability of the touchscreen to ambient surfaces through conductive strips. These systems can support interactions such as touch widgets [10–12], trackpad [3] as well as tangible interfaces [1, 25, 26]. Unfortunately, these approaches can only support applications with very limited sensing range and fabrication materials. Furthermore, the sensing and fabrication methods, as well as the design space of long-range capacitive sensing beyond the touchscreen for interactive applications have not yet been studied.

In this paper, we present *FlexTouch*, a technique for enabling long-range touch sensing interfaces beyond commercial touchscreens leveraging a variety of flexible conductive materials (Fig 1). *FlexTouch* utilizes simple fabrication techniques to create a variety of passive, conductive 2D-patterned touch interfaces that enable new health and wellness applications. Our contributions in this paper are as follow:

1. We enabled large-scale touch sensing up to 4 meters and objects' presence up to 2 meters away from the capacitive touchscreen to ambient surroundings by including the local ground in the external conductive pattern design.

2. We showed that *FlexTouch* is easy to fabricate, assemble and use. The 2D circuit-like pattern is compatible with various conductive materials (copper foil tape, silver nanoparticle ink, ITO frames, and carbon paint), as well as fabrication methods (cutting, coating, and ink-jet printing). Furthermore, we proposed two easy attachment or assembly approaches to connect the extension part to touchscreens.

3. We benchmarked the performance of *FlexTouch* through user studies. Specifically, we fully explored design variables such as materials, extension strips' width as well as gap distance between strips and evaluated their impact on the coverage distance of *FlexTouch*. In addition, we demonstrated the versatility and feasibility of

FlexTouch through applications such as body posture sensing, object presence detection as well as enhanced fitness sensing applications.

2 RELATED WORK

In this section, we first review a set of work that aims to enable touch interaction on everyday surfaces and objects. Then we dive deeper into prior work in the field of capacitive sensing closely related to *FlexTouch* to better position our work in the related literature.

2.1 Touch Interaction on Everyday Surfaces and Objects

Researchers have explored various methods and techniques to enable interactive interfaces on everyday surfaces and objects. One popular method to enable touch interactions is by projecting 2D user interfaces onto a surface and then recognize user interaction via computer vision [2, 21, 29, 30]. These solutions can support large-scale interactions which are suitable for fixed infrastructure. However, its power consumption and form factor are still challenging for everyday mobile scenarios.

Touch interaction can also be supported by acoustic sensing. Researchers have explored recognizing a discrete set of touch events on everyday objects such as windows [20], desktops, and other surfaces [7]. However, these approaches only apply towards a small set of touch inputs like tapping or scratching on various materials.

Another popular method is electromagnetic sensing. *SmartSkin* enabled multi-touch interaction on surfaces using a mesh-shaped capacitive sensor grid [22]. *Electrick* [33] and *Pulp Nonfiction* [32] enabled touch input on everyday surfaces and objects using Electric Field Tomography (EIT) with coated conductive materials on everyday surfaces and objects. *Touche* [23] enhances touch interface on the human body or everyday objects by measuring the electrical profiles with a frequency-sweep signal. *Midas* [24] fabricated customized capacitive touch sensors to prototyping interactive object with a circuit board milling machine. *Wall++* [34] enabled large-scale touch interaction on the wall for activity recognition. Other prior work also explored printing custom-shaped capacitive sensors [4, 16, 17, 28]. These prior works demonstrated very promising results, however, they rely heavily on dedicated sensing platforms and customized embedded systems to provide power supply, external sensors, signal processing, and communication modules. These requirements create barriers for end-users to easily fabricate customized touch interfaces.

2.2 Capacitive Touch Interaction Sensing beyond Touchscreens

Capacitive sensing was introduced into the field of HCI over two decades ago. Recently, Grosse-Puppendahl and his colleagues reviewed and summarized past researches related to capacitive sensing theories and techniques [5]. Among all the capacitive sensing methods, shunt mode sensing is the most widely spread approach in implementing modern capacitive touchscreens. The touch panel consists of multiple layers above the display screen with all the sensing nodes oriented in a row-column matrix. Each node is a high-resolution continuous capacitance measurement sensor. Obtaining the low-level capacitive data from the touchscreen provides us with more capability beyond binary finger touch sensing. Similar to our approach, *BodyPrint*[8] and *CapAuth*[6] combined capacitive touchscreens with machine learning classifiers to provide authentication and even identification of users. *PalmTouch* enabled the palm as an additional input modality to enhance mobile interaction [14]. Researchers also explored the potential of using the raw capacitive data of touchscreens to support sensing of tangible 3D-printed gadgets on top of the screen [1, 25, 26]. While these prior works share the same raw capacitance signal as our approach, we focus on fabricating conductive interfaces to support large-scale, flexible touch interfaces on the ambient surfaces connected to touchscreens.

In close proximity to our work, researchers explored methods extending touch interaction from the touchscreen to ambient objects or surfaces with conductive materials. *Clip-on Gadgets* extended capacitive touchpoints on

the phone to physical controllers via conductive materials [31]. Kato and his colleagues went a step further, fabricating 3D-printed conductive gadgets with haptic feedback patterns [12]. User interaction with these gadgets was detected via the capacitive screen when they were placed onto the phone. In addition, they also presented a technique named *ExtensionSticker* which allowed touch sensing to be transferred to ambient surfaces [10, 11]. However, without accessing the raw capacitive data, *ExtensionSticker* could not support large-scale touch interfaces. Long-range conductive strips attached on touchscreens would be recognized by the built-in touch detector as finger touch events, which prevents the detection of real touches on the strip. As a result, these extension-sticker techniques only allow for near-range touch sensing interfaces. Recently, Gao and Ikematsu demonstrated the feasibility of using 1D conductive ink strips or ABS filament arrays sensing 2D finger positioning [3, 9] through measuring the resistance introduced to the touchscreen's sensing circuit. However, they only demonstrated short-range applications such as 2D finger tracking on phone-based VR headsets or 1D touch bar using a single sensor node.

In contrast with prior work, *FlexTouch* allows users to create large-scale, passive, flexible and customizable touch sensitive gadgets that can be easily attached to the mobile touchscreen for rapid prototyping of interactive applications. We leverage the local ground plane of the touchscreen to boost signal strength enabling touch-sensing coverage range up to 4 meters and objects' presence sensing range up to 2 meters. This allows *FlexTouch* to support large-scale sensing applications such as touch sensitive yoga mats or bed mattresses with signal processing and machine learning techniques. These advancements allow *FlexTouch* to be applicable to a variety of new touch sensing applications beyond the prior work.

3 FLEXTOUCH: WORKING PRINCIPLES

Any conductive object in contact with the touchscreen draws currents passing from the driving line (transmitting electrode) to the sensing line (receiving electrode) at each junction. The control IC of the touchscreen is designed to measure this leaking current to detect touch events. Prior work introduced an extension tape enlarging the transmitting electrode to boost the touch sensing distance [3, 9–11]. In Kato's work, the signal transmitted into the conductive tape returns to the device through an environmental coupling path, called ***virtual ground***. To further extend the capacitive sensing distance, we introduce the ground of the phone, the ***local ground***, into the extended circuit. Therefore, we can short this coupling path with another conductive tape directly passing the signal back to the touchscreen device. Although the local ground can be extended from the charging port, we use the back panel of the touchscreen device since it's easier to assemble as illustrated in Fig 5 C. We can simplify the structure made of the attached conductive tape, the back panel, and the inner local ground circuit as one large capacitor. Here, we define two types of extension strips: 1) ***signal strip***, which is attached to the touchscreen sensor node, and 2) ***grounding strip*** which extends the local ground of the touchscreen.

We present simplified equivalent circuits under each column in Fig 2 with each capacitive sensor node treated as a RC circuit. $R_s, C_m, C_p, C_e, C_f, C_{fg}$,$C_{eg}, R_e$ represent the inner resistance, mutual capacitance, parasitic capacitance, introduced capacitance between the extended element and local ground, touch introduced capacitance, introduced capacitance of touching both the signal and grounding strips, changed capacitance between the extended element and local ground as well as the extended element introduced resistance. Equation (1) shows the calculation of v_{out} ignoring the effect of R_e, using $C_{e(g)}$ representing either C_e or C_{eg} and $C_{f(g)}$ representing either C_f or C_{fg}.

$$V_{out} = v_{in}(1 - e^{-\frac{C_m+C_p+C_{e(g)}+C_{f(g)}}{R_s C_m (C_p+C_{e(g)}+C_{f(g)})} t}) \tag{1}$$

The touchscreen controller transmits a series of step voltage signals to scan through each electrode and measures the charging time (time for V_{out} to reach a threshold) as raw capacitive values of the touchscreen. The

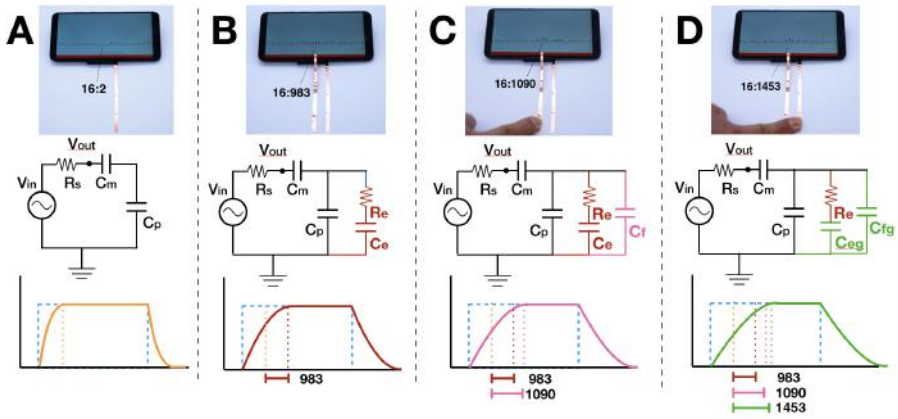

Fig. 2. Four capacitive states and corresponding simplified equivalent circuits of *FlexTouch*. A: Idle state - original touchscreen sensing node. B: Attaching state - adding the signal strip on one touchscreen sensing node. C: Touching state - touch on the signal strip. D: Grounding state - touch both the signal strip and the grounding strip.

charging time is linearly dependent on the Time Constant of the RC circuit, named τ, that is given as:

$$\tau = R_s \frac{C_m(C_p + C_{e(g)} + C_{f(g)})}{C_m + C_p + C_{e(g)} + C_{f(g)}} \tag{2}$$

We assume that C_m and C_p are static with value around $10pF$. The value of C_e depends on the characteristics of the extended surfaces such as conductivity of the material, length, and width as well as the intersection effect between the extended elements. C_f typically varies from several to dozens of pF introduced by human touch.

Fully understanding the effect of C_e is the key to exploring the upper-limit of *FlexTouch*'s performance. In pursuit of testing this limit, we simply model the mutual capacitance between the extended material and the virtual ground with following formula.

$$C_e = \varepsilon \frac{A}{d} = \varepsilon \frac{L \times D}{d} \tag{3}$$

A represents the scale of dimensions of extension strips including length (L) and width (D), d represents the separation between the signal strip and the local ground, and ε represents the material's permittivity of extension strips. Therefore, to fully evaluate the sensing distance capability of *FlexTouch*, we need to study the effect of variable factors contained in the fabrication material along with the width and gap distance of the extension strips.

4 FLEXTOUCH IMPLEMENTATION

To validate the feasibility of our approach across different Android devices, We implemented *FlexTouch* on a Huawei P20 and a Huawei P10 phone. By rooting the Android operating system and modifying the driver of the touch screen controller IC in the kernel's source code, we extracted the raw capacitive sensing data: $32 \times 16 = 512px$ 16-bit diff value image across a 5.8-inch surface at 100 fps for Huawei P20 phone, $28 \times 16 = 448px$, 16-bit diff value image across 5.1-inch surface area at 20 fps for Huawei P10 phone. We built an Android application that shows positions and raw capacitive values with corresponding update rates of chosen sensing nodes. The app also logs the raw capacitive image to a local server for later analysis.

4.1 Signal Processing for Touch Event Detection

In this section, we use the P20 phone as an example to present the signal processing and the touch event detection pipeline of *FlexTouch*.

Fig 3 demonstrates the signal processing procedure to detect the touch event on a 3-meter extension tape attached to the touchscreen. To filter out the high-frequency background noises, we applied a moving-average filter on the raw capacitive data using the unweighted mean of the previous 10 data points. During a touch event, a sharp signal rise occurs. To detect these rising step events, we applied a sliding window that contains 20 data points on a low-pass filtered signal. The step event can be extracted by comparing the data samples in front of the sliding window queue and at the tail of the queue. Each data sample in the black line graph in Fig 3 is calculated using the following equation where S_i represents the filtered capacitive data.

$$S_{diff} = \frac{S_{16} + S_{17} + S_{18} + S_{19}}{4} - \frac{S_0 + S_1 + S_2 + S_3}{4} \tag{4}$$

Here we define the ***signal-to-noise ratio (SNR)*** representing the signal strength of the raw capacitive data. As shown in Fig 3, we define the ***Noise*** to be the difference between the maximum and minimum values of 100 data points for P20 before the touch event. The ***Signal*** is the S_{diff}. To extract the touch signal from the background noise effectively, the SNR should be greater than a predetermined threshold. In theory, if SNR > 1, we can detect touch events.

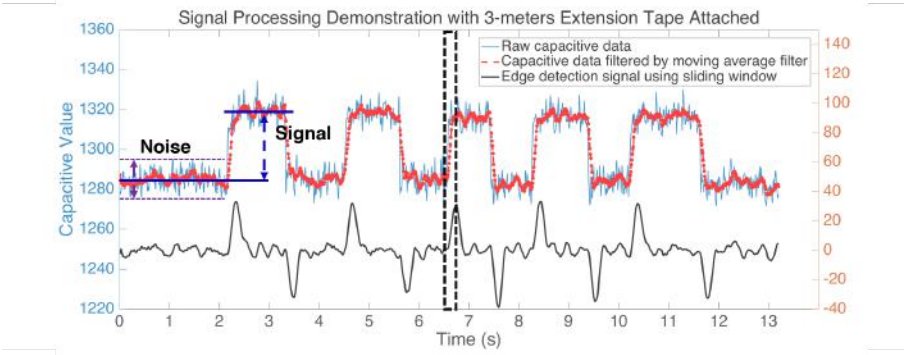

Fig. 3. Signal processing demo detecting the touch event.

4.2 Fabrication

We identified materials that can be easily customized into everyday surfaces with properties including flexibility, conductivity, and commercial availability. We fabricated interfaces using these materials through various processes, including adhering, cutting (e.g., manual cutting, laser cutting) and coating methods (e.g., ink-jet printing, brush painting). We leveraged the following materials to fabricate *FlexTouch* interfaces.

4.2.1 Conductive Tapes. Conductive adhesive tapes are widely used for electromagnetic shielding and transmission wiring (e.g. paper circuits). The most widely available conductive tape is an adhesive copper foil tape that can be found at most hardware, electronic or gardening stores (Fig4 A). It is $2.50 per roll (6.3 mm x 20 m). The copper tape is highly conductive on both sides (0.05 Ω per square centimeter).

End-users can manually arrange any layout on any surface using copper foil tapes (e.g., Fig 4 E) without any additional fabrication equipment. In addition, the conductive tape is more flexible and suitable for large-scale

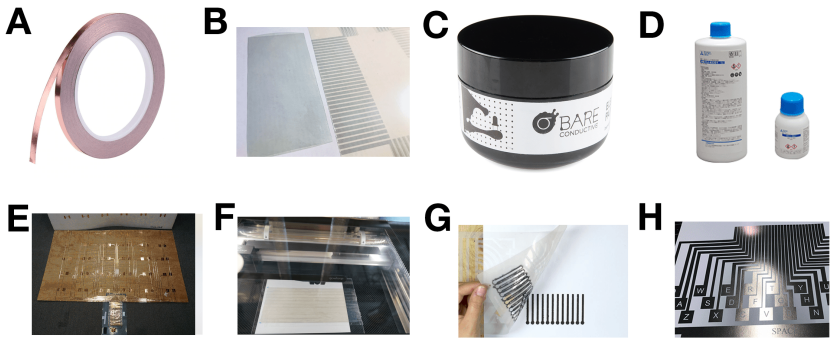

Fig. 4. Commercially available materials. Copper foil tape (A) can be fixed to any surface (E). ITO PET Plastic film (B) can be fabricated to any 2D pattern using a laser cutter (F) or manually. Bare conductive carbon paint (C) and screen painting (G). Ink-jet circuit printer with Mitsubishi Silver nanoparticle ink (D) for printable conductive 2D layout (H).

applications since it can easily adhere to everyday objects. However, the copper foil tape is not suitable for volume production since it is not compatible with current fabricating techniques such as laser cutting or printing.

4.2.2 Conductive Films. Film-like materials can be subtracted to 2D patterns using cutting or etching fabrication methods. One example material is the flexible Indium Tin Oxide (ITO) coated PET plastic film that is semi-transparent and conductive. We use the commercially available ITO-coated PET film manufactured by HNXCKJ [27] that is compatible with laser cutters. Furthermore, 2D custom layouts are also available by coating ITO materials on extremely thin ($0.05mm$) plastic film at a cost of $30 per square foot (Fig 4 B).

Since the ITO-coated PET plastic film is highly transparent, it can be attached to the touchscreen without occluding the display (Fig 5 A). The ITO film can be customized as a screen protector for daily use with an array of ITO strips attached to the edges of the screen. This ITO strip array interface can be connected to the external application easily with a plug and play design as Fig 5 A and B show.

4.2.3 Conductive Coating. Liquid paint coating and ink printing are more versatile, as they can be added onto any surface in post-production. We identified two coating materials as examples. We use conductive carbon paint from Bare Conductive (Fig 4 C, $280 per litter). This material can be painted on a flat surface such as a wooden board or cardboard, and then laser cut to engrave the layout on top of it. Another suitable coating material is printable ink. We identified Silver nanoparticle ink made by Mitsubishi (Fig 4 D, $340 per 100 ML) as presented by Instant Inkjet Circuits [13]. We fabricated the inkjet printable circuit with a Brother MFC-J480DW model printer.

The conductive coating method is compatible with mass production due to its reproducibility. However, because of the limited size of each template or substrate, we need to further assemble the fabricated elements for large-scale application.

4.3 Plug and Play

In this section, we present *FlexTouch*'s plug and play interface for daily use by proposing two assembly approaches as demonstrated in Fig 5.

- **Adhere the external application with an ITO array film.** The ITO film is suitable for being integrated into a screen protector with an ITO conductive array connected to the edge of the touchscreen. The adhesive ITO film can easily be attached or detached to the external 2D patterned application.

- **Fix the external application on the phone's edge with a clip.** The external application is connected with an array of conductive threads on one side of the clip while the electrodes on the 2D pattern representing the local ground are connected on the other side of the clip as shown in Fig 5 C. The customized part can be clipped onto the edge of the touchscreen as shown in Fig 5 D.

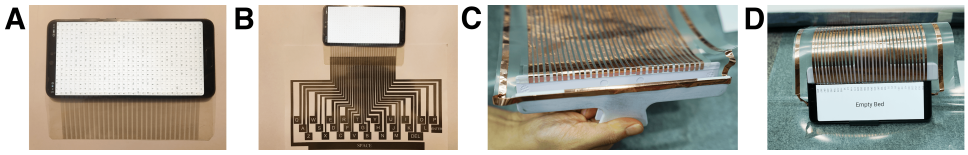

Fig. 5. Demonstration of two assembly methods. The ITO strip array interface (A) can be stuck to a 2D-patterned application (B). The external application can be clipped onto the edge of the touchscreen (C and D).

5 FLEXTOUCH SENSING CAPABILITY EVALUATION

In this section, we evaluate the sensing range of *FlexTouch* considering the effects of several factors including fabrication materials, the signal strip's dimension, sensing hardware and the configuration of the grounding strip.

5.1 Evaluating Sensing Range with Variable Fabrication Material, Hardware, and the Local Ground

Fig 6 illustrates our hardware setup for this study. Two strips are coming out from the phone. The signal strip is directly attached to the phone touch surface by a plastic clamp, while the grounding strip is connected to the back plate of the phone. In this study, we only look at the difference between using and not using the grounding strip. We discuss other variables pertaining to the grounding strip in a more thorough study in later parts of this section.

Fig. 6. Experiment setup to evaluate the touch sensing coverage range.

To evaluate the effect of different materials, We fabricated four different 5-meter long signal strips using materials including copper foil tape (CFT), ITO PET film (IPF), carbon paint (CP), and silver nanoparticle ink (SNI) with a fixed width of 1.5mm. We set the grounding strip (5-meter long, 6mm-wide copper foil tape) 2cm away from the signal strip in this study. We recruited four participants for this experiment with an average age of 26.5 (SD = 2.5). The study lasted for 2 hours in total and we compensated each participant with a $50 dollar gift card.

1) We attached the signal strip to the central position of the 8th sensing node on the touchscreen's left edge at the beginning of each session. In each session, we randomly selected two participants to perform a one-second finger touch on the far end of the signal strip five times followed by a one-second finger touch on the far end of both the signal and the grounding strips (also five times). Then we attached the signal strip to the 18th sensing node and repeat above procedure.

2) We switched the phone hardware and repeated step 1).

3) We cut both signal and grounding strips to the next neighboring length following the order of 5m, 4m, 3m, 2.5m, 2m, 1.5m, 1m, 0.5m, 0.25m and 0.1m in sequence and repeated steps 1) and 2).

4) After completing the test on one material, we replaced it with another signal strip made of different material and repeated the experiment. Participants took a two-minute break between material switches.

Length[m]	**0.10**	**0.25**	**0.50**	**1.00**	**1.50**	**2.00**	**2.50**	**3.00**	**4.00**	**5.00**
P20, CFT	6.8	3.5	1.6	1.1	0.6	-	-	-	-	-
P20, IPF	6.6	3.4	1.4	0.9	0.5	-	-	-	-	-
P20, CP	6.5	3.1	1.9	0.8	-	-	-	-	-	-
P20, SNI	6.4	2.9	1.3	0.9	-	-	-	-	-	-
P20, CFT w/ GND	15.8	9.8	5.8	4.7	3.3	2.6	2.0	1.5	1.3	0.7
P20, IPF w/ GND	16.5	10.8	5.5	4.0	3.1	2.0	1.6	1.1	0.8	0.5
P20, CP w/ GND	15.4	10.1	6.0	3.7	2.2	1.7	1.0	0.8	-	-
P20, SNI w/ GND	15.3	9.8	5.4	3.1	2.2	1.7	1.4	1.2	0.9	0.5
P10, CFT	15.7	7.6	4.3	2.7	1.7	1.1	0.7	-	-	-
P10, IPF	14.2	7.5	3.9	2.9	1.4	1.0	0.5	-	-	-
P10, CP	14.4	6.8	3.2	1.6	0.8	0.5	-	-	-	-
P10, SNI	14.9	6.9	3.1	2.8	1.4	1.0	0.6	-	-	-
P10, CFT w/ GND	20.4	10.2	7.0	4.3	3.1	2.3	1.9	1.5	1.1	0.8
P10, IPF w/ GND	21.4	11.5	7.9	5.3	3.2	2.7	1.7	1.2	0.8	0.5
P10, CP w/ GND	20.1	12.4	8.1	4.3	2.8	2.1	1.2	0.7	-	-
P10, SNI w/ GND	19.4	11.2	8.6	4.1	2.8	2.0	1.6	1.2	0.8	0.5

Table 1. Average SNR versus extension distance under different configurations. (CFT: copper foil tap, IPF: ITO PET film, CP: carbon paint, SNI: silver nanoparticle ink)

5.1.1 Results. We summarize our results in Table 1, which outlines the signal strength illustrated by the SNR value of our system. There are a total of 16 different hardware/material/grounding strip's presence configurations and each of them has ten different signal strip length configurations. We highlight the following insights gained from this evaluation study:

1. *FlexTouch* can support large-scale capacitive sensing applications with a coverage range of up to 4 meters. Using the threshold of SNR > 1, we observe that the minimum sensing distance supported by *FlexTouch* exceeded 0.5 meters regardless of the hardware, the material, and the grounding strip's presence. However, the grounding strip helps extend the sensing range significantly: Under the best conditions, with both the p10 and p20 hardware and CFT material, *Flextouch* could reach coverage distance of more than 4 meters.

2. *FlexTouch*'s sensing range is positively correlated with material conductivity. Among the four materials, CFT achieved the longest sensing range, following by SNI and IPF, finally by CP. This ordering is consistent with the conductivity ordering of the 4 materials presented in Figure 7 B. We believe that materials with even better conductivity may be able to exceed the sensing range we observed in this study.

3. The extension distance increases as the width of the signal strip decreases. To better understand the effect of the width of the signal strip, we conducted a follow-up study changing the width of the signal strip made with 4 different materials with a fixed length of 3 meters. We recorded the SNR in Figure 7 A, which demonstrates that *FlexTouch* has the best performance with a 1.5*mm*-wide signal strip regardless of the fabrication material. We believe that even thinner strip will be able to support longer sensing ranges. However, since a thinner strip is less conductive, we believe that there's a lower limit on the strip's width.

A

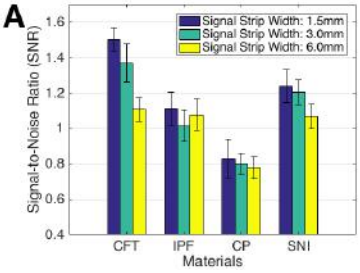

B

Length[m]	0.10	0.25	0.50	1.00	1.50
CFT	0.4	1.1	2.1	5.4	6.0
IPF	0.8K	1.8K	4.0K	7.7K	11.5K
CP	2.6K	6.5K	11.0K	24.4K	38.5K
SNI	0.3K	0.8K	1.6K	3.0K	4.7K
Length[m]	**2.00**	**2.50**	**3.00**	**4.00**	**5.00**
CFT	11.4	14.2	17.4	22.5	29.8
IPF	15.2K	19.1K	23.0K	30.5K	37.5K
CP	55.4K	65.1K	79.6K	120.3K	154.6K
SNI	6.2K	7.7K	9.6K	12.6K	15.9K

Fig. 7. The SNR versus the signal strip width using four different materials (A). The table of material's resistance values (Ω) under different extension lengths (B).

4. *FlexTouch* can not differentiate touchpoints at different locations on the extension strip with the presence of the ground plane. We evaluated the touch resolution on a single pair of extension strips by touching on different positions with a 50*cm*-step using different materials. We did not observe that 2D touch input could be enabled with single-layer conductive materials as prior work [3, 9] mentioned with the grounding strip's presence.

5. No significant difference in using different capacitive sensing hardware. The 2 different phones being employed in our study, Huawei p10 and P20 demonstrate moderate SNR difference when the same material is being deployed with a length below 1*m*. However, when the strip length continued to increase, the SNR demonstrated similar results when all other variables are consistent. Given limited hardware resources, we were only able to evaluate these two phone models. Future studies that include capacitive touchscreens from different manufacturers will be necessary to fully understand the impact of capacitive touchscreens on the feasible sensing range of our system.

5.1.2 Study Results in Relation to the Proposed Working Principle. Results in Table 1 show that as the length of the sensing strip increases linearly, the touch signal strength decreases logarithmically. As presented in section *FlexTouch: Working Principles*, the finger touch introduces additional shunt circuit changing C_e to C_{eg}. We assume the values of C_f, C_m, C_p are 5 pF, 10 pF and 10 pF while $C_{eg} = 1.5 \times C_e$. Then Formula (2) can be presented as following.

Before the touch event:

$$\tau_b = a\frac{100 + 10C_e}{20 + C_e} \tag{5}$$

After the finger touch on the signal strip only as well as on both the signal strip and the grounding strip:

$$\tau_{af} = a\frac{150 + 10C_e}{25 + C_e}, \tau_{ag} = a\frac{150 + 15C_e}{25 + 1.5C_e} \tag{6}$$

The estimated capacitance value can be represented as:

$$\tau_{df} = \tau_{af} - \tau_b, \tau_{dg} = \tau_{ag} - \tau_b \tag{7}$$

We assume that $C_e = 100 \times L$ where L represents the length (meter) of the strip since the width is assumed to be static. The curve of how the estimated capacitive value along the strip length matches the measured raw data if a is assigned to 600. The pattern we see in our result matches with the model we built for explaining *FlexTouch*'s working principle.

5.2 Understanding the Effect of the Grounding Strip

The previous study shows the significant effect of introducing the grounding strip into the extension circuit design. There are additional variables such as the distance between the grounding strip and the signal strip, the width of the grounding strip as well as the material of the grounding strip that we would like to further evaluate to provide in-depth insights into designing touch sensing solutions with *FlexTouch* in this section.

5.2.1 Effect of the Gap Between Grounding and Signal Strips. We used copper foil tape as example material to examine the effect of the gap between the grounding strip and the signal strip on the maximum touch sensing distance. We set the grounding strip's width to be 6*mm*. We measured the maximum coverage with the following variables. 1) Gap distance between the central lines between the signal and grounding strips: 0.5*cm*, 1*cm*, 2*cm*, 3*cm*, 5*cm* and 10*cm*. 2) Signal strip's width: 1.5*mm* and 3.0*mm*. 3) Touch postures: single index finger touch and dual index finger touch with two hands.

To measure the maximum touch sensing distance, we started with the maximum sensing distance measured in the previous study. In each session, we increased/decreased the extension distance by sticking/cutting additional n pieces of 10*cm*-long copper foil tape at the far ends of both the grounding and signal strips. We recruited four participants for this study with an average age of 25.5 (SD = 1.5). They performed three touches with each touch posture at the far ends the extension strips. We repeated the above sessions until the SNR exceeded 1.0 for both single-finger and double-finger touches. We repeated the above procedure five times to obtain an average coverage distance for each condition.

1. The maximum touch sensing distance increases logarithmically as the gap distance between the grounding strip and signal strip increases. As shown in Figure 8, there exists an upper limit on the touching sensing coverage distance around 5 meters regarding the gap distance and the signal strip's width. However, although larger gap distance results in better sensing coverage distance, it limits the number of strips that can be deployed for any given space.

2. Touch posture has no significant effect on the coverage distance performance. There is no significant difference between touches with one finger or two fingers from two hands ($F_{1,89} = 0.32, p = 0.54$). We envision that future work could connect the local ground directly to users and not to the extension circuit, enabling longer sensing range and higher resolution design.

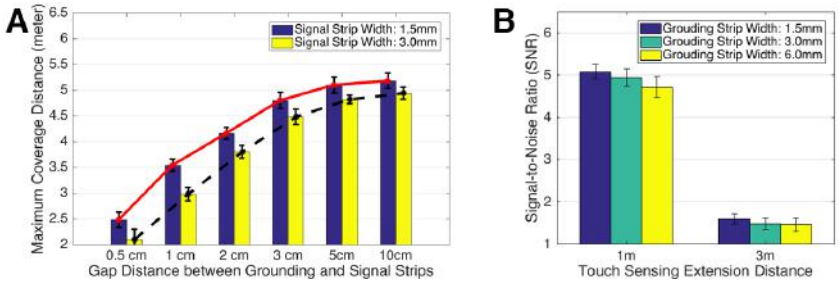

Fig. 8. Maximum touch sensing distance versus the gap distance between signal and grounding strips (A). SNR versus the grounding strip width with different extension distances (B).

5.2.2 Effect of Grounding Strip Width. We used copper foil tape as example material to examine the effect of the grounding strip width on the touch sensing distance. We set the gap distance between extension strips to be 2*cm* and the signal strip width to be 1.5*mm*. We measured the signal strength on fixed extension distances (1*m* and 3*m*) with different grounding strip's width: 1.5*mm*, 3.0*mm* and 6*mm*. We recruited four users to touch the far

ends of the paired extension strips three times for each condition. We repeated the above procedure five times to obtain an average measured SNR. We highlight the following insights gained from this evaluation study:

The touch sensing coverage distance is negatively correlated with the grounding strip's width. We recorded the SNR values in Figure 8 B, which demonstrates that *FlexTouch* has the best performance with the 1.5*mm*-wide signal strip. We recommend a thinner signal strip that can support better sensing range performance as well as higher resolution design. Combined with the result on the signal strip's width in Section 5.1.1, we believe that the sensing distance can be further extended if we adopt 1.5*mm*-wide or thinner copper foil tape for both the signal and grounding strips.

5.2.3 Effect of the Grounding Strip Material. In this study, we explored whether grounding strip material affects the sensing distance performance. We set the signal strip material to be copper foil tape, the gap distance between extension strips to be 2*cm* and the widths of both the signal strip and grounding strip to be 6.0*mm*. We measured the SNR values of 1-meter and 3-meters sensing distance with four different grounding strip's materials. The result is illustrated in Table 2.

Material	**CFT**	**IPF**		**CP**		**SNI**	
Condition	**reference**	**ground**	**signal**	**ground**	**signal**	**ground**	**signal**
1*m* sensing distance	1.14 (0.07)	1.06 (0.11)	1.07 (0.13)	0.88 (0.12)	0.86 (0.10)	1.11 (0.14)	1.09 (0.13)
3*m* sensing distance	3.40 (0.20)	3.31 (0.25)	3.35 (0.23)	3.22 (0.12)	3.20 (0.08)	3.42 (0.13)	3.37 (0.14)

Table 2. Average (standard deviation) SNR values with one strip made of CFT and the other made of one of the three materials.

1. *FlexTouch* sensing range is positively correlated with material conductivity of the *grounding strip* in general. Similar to the results in Section *5.1.1*, we found that the material conductivity has a positive effect on the sensing range performance.

Then we switched the grounding strip and the signal strip which are made of different materials and noticed that:

2. Signal strip and ground strip made of different materials are interchangeable when they have the same width. We found no significant difference in the signal strength when switched the two strips with the same width but different materials.

5.2.4 Study Results in Relation to the Proposed Working Principle . Section 5.1.2 explains the relationship between signal strength and the extension strip's length using the working principle hypotheses in Section 3. We explain the results we found in study 2 that pertain to the effect of separation - d as well as fabrication material - ε.

To enhance the effect introduced by touch, less capacitance between the signal strip and the grounding strip is preferred, which is represented as C_e. The sensing distance can be represented as:

$$L = \frac{C_e \times d}{\varepsilon \times D} \tag{8}$$

Therefore, we conclude that smaller extension strip width (D), larger gap distance (d), more conductive material and more insulating material between strips (smaller ε) will help extend the sensing range, which is consistent with our study's results.

5.3 Evaluating Object Presence Sensing Capabilities

Given the capacitive nature of *FlexTouch*'s sensing principle, it can go beyond sensing touch events. Everyday objects that contain capacitance also draw electric current from the touchscreen and can be detected by *FlexTouch*. In this section, we evaluate the feasibility of detecting everyday objects' presence using *FlexTouch*.

5.3.1 Apparatus and Procedure. In this study, we used 3.0*mm* wide copper foil tape and a Huawei P20 phone. We explored a range of factors that may affect *FlexTouch*'s capability in sensing everyday objects' presence: the dielectric property and materials of different everyday objects, the length of the extension strips as well as the presence of the local ground. We used the following procedure in the experiment:

1) We attached the signal strip to the central position of the 19th sensing node on the left edge of the touchscreen. Then we started the testing application on the phone sending the raw capacitive data to a local server running on a laptop for later analysis.

2) We placed 11 pre-selected objects in random order at the end of the signal strip without the grounding strip's presence for around 2 seconds then on both the signal and grounding strips for another 2 seconds. We picked up and re-placed the object five times, ensuring the object was in contact with the strips on each placement.

3) We trimmed the strips in order of the following lengths: 3m, 2m, 1.5m, 1m, 0.5m, 0.25m, 0.1m and repeated step 2).

5.3.2 Results. Table 3 presents the average SNR value with 22 configurations across everyday objects and the presence of the grounding strip.

As presented in Table 3, *FlexTouch* can sense the presence of everyday objects by detecting the current they draw via the extension strip. The second column in Table 3 illustrates that all the objects change the capacitive signal extended from the touchscreen on the phone. However, the sensing range varies with the object's material. Objects made of metal have the strongest signal strength. The coverage distance ranges from 50*cm* to 2*m*. Besides, pairing the local ground with the touch screen extension strip can dramatically enhance the object detection's sensing range.

Length[m]	**0.10**	**0.25**	**0.50**	**1.00**	**1.50**	**2.00**	**3.00**
Finger Touch (**reference**)	15.8/6.8	9.8/3.5	5.8/1.6	4.7/1.1	3.3/0.6	2.6/-	1.5/-
$5cm \times 5cm$ Copper Foil Tape	15.3/3.2	9.5/1.9	5.5/0.8	4.6/-	3.0/-	2.3/-	1.3/-
Stainless Steel Water Cup	12.6/3.4	10.0/2.0	4.3/1.1	2.0/-	1.6/-	1.5/-	0.7/-
MacBook Pro 13'	5.4/2.4	3.7/1.7	1.2/0.6	0.6/-	-/-	-/-	-/-
Carving Knife	5.6/1.5	2.7/0.6	1.3/-	-/-	-/-	-/-	-/-
iPhone XR	4.6/2.5	2.5/2.0	1.2/0.5	0.7/-	-/-	-/-	-/-
550 ml Bottled Water	4.3/2.8	2.8/1.2	0.6/-	-/-	-/-	-/-	-/-
50 ml Bottled Water	3.1/1.3	2.0/0.7	-/-	-/-	-/-	-/-	-/-
Glass Cup	2.7/0.6	1.0/-	-/-	-/-	-/-	-/-	-/-
Notebook	0.9/0.8	-/-	-/-	-/-	-/-	-/-	-/-
Cardboard Box	0.5/0.6	-/-	-/-	-/-	-/-	-/-	-/-
Mouse	0.5/0.5	-/-	-/-	-/-	-/-	-/-	-/-

Table 3. Average SNRs versus extension strips' lengths with different everyday objects. The table's X and Y values (X/Y) represents the SNR values of conditions with and without the grounding strip.

6 EXAMPLE APPLICATIONS

In this section, we present four example applications to demonstrate the versatility of *Flextouch*, including examples of body posture recognition, 2D large-scale continuous touch tracking as well as sensing the presence of everyday objects. These applications demonstrate the possibility of new interaction methods and the sensing potential of *FlexTouch*.

6.1 Smart Mattress for Sleep Monitoring

As *FlexTouch*'s sensing range can reach up to 4 meters, we can leverage this long-range capability to detect users' behaviors while they're in bed. This is achieved by fabricating a three-layer structure with $5 \times 6 = 30$ sensing notes as presented in Fig 9 A - C. Each sensing node on the top layer is formed with a signal and a grounding electrode (Fig 9 B). All electrode pairs are connected to electrodes on the bottom layer. We placed a mattress on a wooden board and affixed a copper-tape circuit (Fig 9 C) with its electrodes connected with the electrodes on the bottom layer of the mattress. We activated the application by plugging in the touchscreen phone using a clip with an array of copper foil tapes attached (Fig 9 E to I). The material cost of this application was 10 USD.

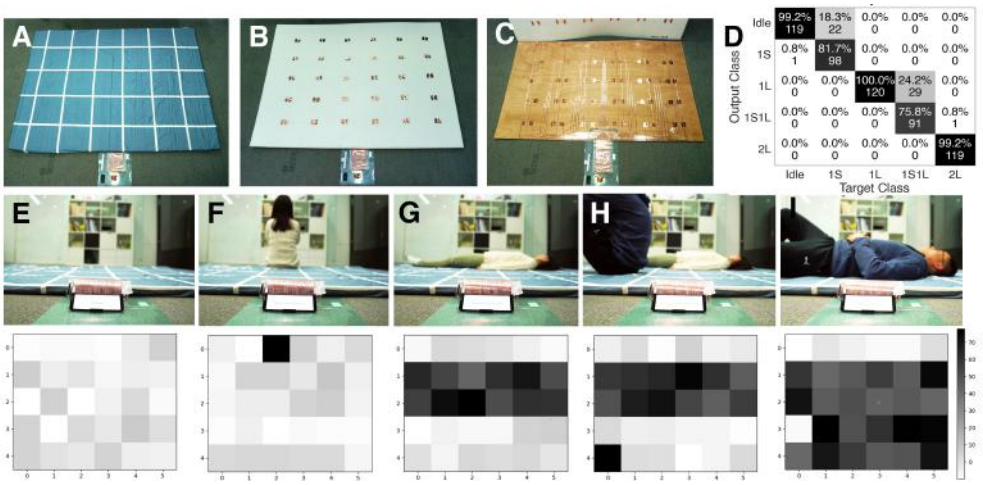

Fig. 9. The structure of the smart mattress (A - C), the classification confusion matrix (D) and the five detected states (E - I) with corresponding scenarios and raw sensing data visualization

6.1.1 User Evaluation. To evaluate the performance of the smart mattress, we recruited eight pairs of participants (10 males) with an average age of 25.6 (SD = 2.2) and an average height of 170 cm (SD = 5.3) who we compensated with a $20 gift card for a 30-minute test. There was one practice session followed by three data collection sessions. For each session, the paired participants followed the instruction of *single user sitting on the bed*, *single user lying on the bed*, *one user sitting and one user lying on the bed*, *two users lying on the bed* in order. The paired participants repeated the above procedure in each session five times and kept each posture for approximately 4 seconds. We logged the raw capacitive data with a Huawei P20 phone and logged the procedure with a camera for labeling.

6.1.2 Result. All samples were manually labeled according to the video. We picked frames out of the series of data for each state. The dataset contains 120 data samples per posture across participants and each data sample includes 30 raw capacitive data points. The dataset was randomly split into 2 subsets (96 training samples and 24 testing samples). We conducted 5-fold cross-validation using the LibSVM classifier and achieved an average accuracy of 91.2% across 5 states. We believe that the low resolution causes low recognition when users are sitting on the mattress, as Fig 9 D indicates. We discuss this result and future design recommendations in the later discussion section.

6.2 Smart Yoga Mat for Fitness Posture Detection

The sensing range of *FlexTouch* allows us to enable large-scale sensing applications such as a yoga mat. *FlexTouch* can detect and classify different user poses based on their capacitive profiles when working out on the yoga mat.

Leveraging this functionality, smart home applications can adjust the surrounding environment based on users' physical activities. For instance, it could adjust ambient light, temperature, and music according to the user's activity on the yoga mat. The materials we used to build the touch-sensitive yoga mat cost just 8 USD.

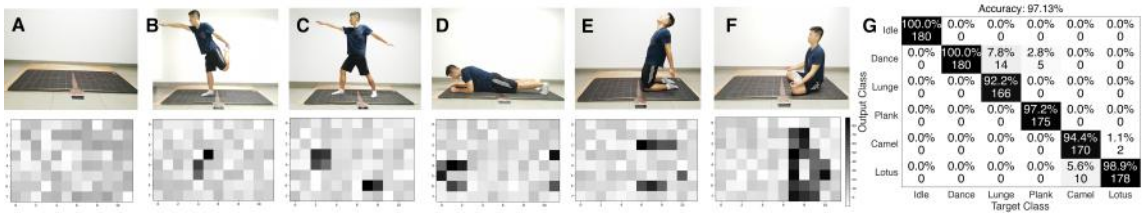

Fig. 10. Recognizing user's posture on the yoga mat built by *FlexTouch* with raw sensing image data

As shown in figure 10, we built a 2D-patterned matrix ($8 \times 11 = 88$ sensing nodes) on a regular yoga mat using ITO strips, which can classify five different yoga poses (lord of the dance pose, plank, high lunge variation, camel pose and lotus pose).

6.2.1 User Evaluation. User Evaluation. We recruited 12 participants (6 males, 6 females, average age 27.7 (SD = 3.4), average height 171.2 cm (SD = 9.8). Each participant received $10 for participating in this study, which included 1 practice session followed by three data collection sessions. Before each data collection session, the five postures were randomized. Then the participant performed each posture five times with a duration of 3 seconds. We logged the raw capacitive data with a Huawei P20 phone and logged the procedure with a camera for ground truth labeling.

6.2.2 Results. All samples were manually labeled according to the video. We picked the middle frame out of the series of data when the pose was performed. The dataset contains 180 data samples in total and each data sample includes 32 frames of raw capacitive data. We performed 5-fold cross-validation on the dataset (144 training samples and 36 testing samples for each iteration) using the LightGBM classifier and achieved an average accuracy of 97.1% across 6 classes (five body postures and no action).

6.3 Fitness Tracking on Count of Repetition, Speed and Distance

In this example, we demonstrate fitness tracking applications when deploying *FlexTouch* on a treadmill, cycling machine, and chest-press machine as shown in Figure 11. Even though some recent commercial fitness machines have the function of sharing data to personal mobile devices, many machines are not embedded with this function such as chest press machine, lat pull-down gym machine, etc. Since these machines have similar periodic patterns, we propose these applications to inspire future designs by identifying the position where the sensing node is placed to sense states, state-changing events, and state-changing speed. We designed a binary sensor using a pair of $1.5m$-long, $3mm$-wide copper foil tapes. Since the update rate of the Huawei P20 phone is 100 fps, the button sensor can detect not only the binary touch event but also how fast it changes. By counting the touch event frequency, we can calculate the distance or speed. This allows users to track their fitness behavior across devices at home or in the gym by simply plugging their phones into a customized passive module. Based on the tracking data, the application can customize fitness plans for individuals. This design cost 0.3 USD.

6.3.1 User Study. To evaluate the tracking accuracy, we recruited six users (3 females, average age of 24.7 (SD = 0.8)). Each user finished three rounds of testing. For each round, users ran on the treadmill for 2 minutes with a maximum speed of $12KM/H$, rode the cycling machine for 2 minutes with a maximum speed of $25KM/H$, and, finally, finished the round with ten chest presses. The study lasted for 20 minutes and we compensated each

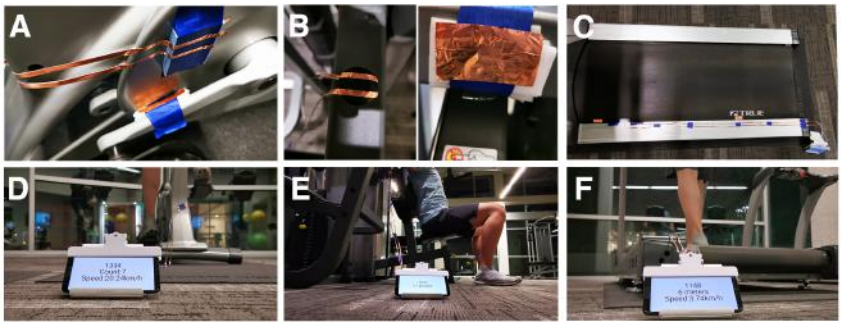

Fig. 11. Fitness tracking using *FlexTouch*. A and D: speed tracking on a cycling machine. B and E: push counter on a chest-press machine. C and F: distance and speed tracking on a treadmill.

participant with a $20 dollar gift card. We used a camera attached on the display panel to record the speed and distance data from the fitness machine for ground truth annotation.

6.3.2 Results. We measured the maximum riding speed from the cycling machine, the maximum running speed and distance resolution from the treadmill as well as repeat counts from the chest-press machine. Since the signal processing algorithm stated in Section 4.4 requires a minimum of 10 valid data to detect a touch event, there's an upper limit of the build button sensor's working frequency under 10 fps. Results indicate that *FlexTouch* had an accuracy of 98.9% on tracking the running and cycling speed and 100% on tracking the chest-press count. Since the touch event happens once every cycle, our distance tracking resolution for the treadmill is 1.5 meter for the model that we tested.

6.4 Smart Desk Reminder Application

Given the flexible and passive nature of *FlexTouch*, we recognize the potential to integrate it into large surfaces such as tables or desks to detect interaction with humans or everyday objects (Fig 12). In this example, we placed three sensing nodes 40*cm* away from the touchscreen to sense the user's body contact as well as one sensing node with 20*cm* distance to sense the cup's water status (i.e. the amount of water remaining in the cup). When the user is working, instead of placing the phone on the desk, the user uses *FlexTouch* to activate the smart desk application. It can remind users to take a break or stay hydrated by drinking water while they work continuously for a while. This is achieved by extending the touch sensing node to the desk where users lay their arm and place the water cup. The material cost for building this application was 0.30 USD.

Fig. 12. Smart desk example detecting user and object's presence and status

6.4.1 User Study. To evaluate the sensing performance on the presence and status of the user and the water cup, we conducted a user study in which six users (2 females, 4 males, average age of 25.0 (SD = 0.9)) participated. For each round, users read a book with his or her arms laying on the table for 20 seconds and then replaced the thin

plastic water cup filled with 250*ml* water with another water cup filled with 50*ml* water. Finally, the user left the desk for 10 seconds and came back to repeat the session five times in total.

6.4.2 Results. We obtained a dataset containing 16 minutes of user's behavior data (96.5*K* data frames). We manually labeled the data to extract 60 data points on user presence status and 90 data points on the cup status. We measured the detection accuracy by whether the user was present as well as the cup's water status (not present, 50*ml* and 250*ml* water inside). Results show that *FlexTouch* can achieve an accuracy of 98.3% on in detecting the user presence at the desk, an accuracy of 92.2% on the cup water status (see the confusion matrix in Figure 12) C.

7 DISCUSSION AND FUTURE WORK

FlexTouch enables large-scale interaction sensing beyond the spatial constraints of capacitive touchscreens by introducing the local ground into the extension circuit design. We show that our technique is compatible with a variety of conductive materials as well as fabrication methods. *FlexTouch* supports posture recognition, human-object interaction as well as enhanced fitness training experiences with a large coverage range of up to 4 meters. In this section, we discuss our findings, design guidelines, and future work.

7.1 Lower Development Barriers Using *FlexTouch*

Since *FlexTouch* requires no external or internal hardware modifications, our technique allows end-users to design and develop varied, low-cost capacitive sensing applications easily with a single touchscreen device. In addition, they can fabricate the customized low-cost interface with various commercially available materials and fabrication methods.

7.2 Effectiveness and Limitation of Introducing the Local Ground to Boost the Sensing Range

FlexTouch enables long-range capacitive sensing of up to 4 meters by introducing the local ground of the touchscreen to the extension circuit design. Through a series of studies, we proved the effectiveness of this approach. In addition, we found some insightful results that may benefit future designs. We recommend thinner, more conductive material to make extension strips and wider gap distances between grounding and signal strips to achieve a better sensing performance.

However, the limitation of this "local ground" method is the low spatial resolution and the effort to avoid overlays between the signal and grounding strips. Designers can choose to increase the resolution by shortening the gap distance and reducing the sensing range. We recommend a multi-layer design to avoid the intersection between signal and grounding strips as Section 6.1 and 6.2 shows. One potential solution to this limitation is connecting users or objects to the local ground directly with conductive threads. Another possible solution is connecting the local ground to the earth ground through a charging line. Therefore, the environmental virtual ground couples the human body and earth ground to the local ground of touchscreen devices.

7.3 Fabrication and Assembly

We demonstrated that *FlexTouch* is compatible with four commercially available fabrication materials as well as a variety of fabrication methods. The current fabrication of our system is primarily based on hand-made prototypes. Additional machine-based approaches are expected for volume production with better quality control. We propose several potential directions for fabrication such as conductive inkjet printing, laser cutting with conductive frames, or printing robots that can enable large-scale circuit design on a wall [1]. Programmable sewing

[1] https://scribit.design/

machines can extend FlexTouch applications to touch interface widgets on a sleeve for quick access to a phone placed in a pocket.

In addition to our existing plug and play approaches in Section 4.3, we expect additional approaches to further extend this idea. For instance, future design can enable an electrode base where users can lay their phone with the touchscreen facing downward to connect to *FlexTouch* interfaces. Furthermore, since the conductive strip increases the raw capacitive value when it's attached to the touchscreen, we can connect different applications with a patterned strip array. *FlexTouch* can detect the signal pattern caused by the patterned strip to serve as a short for launching applications when users attach the extension circuit to the touchscreen.

We recommend future fabrication designs considering the layout and spatial resolution when placing sensing nodes. An improper design leads to low recognition accuracy result as section 6.1 (smart mattress) demonstrates. The distance between sensing nodes is approximately 30 cm. As a result, it is hard for this application sensing users' sitting posture when they sit in the gap between electrodes or on the edge of the mattress. We believe that a higher resolution will improve accuracy significantly. In addition, we observed the negative effect of cloths on the signal strength especially with the presence of the sheet. Therefore, future designs should also consider the object/cover placed between human bodies and the extension surface.

7.4 Enabling More Sensing Nodes

Currently, only the sensing nodes on the edge of the touchscreen have been used (94 nodes for the P20 phone and 88 nodes for the P10 phone). In the future, we can extend more nodes with a cover (Fig13) that can be attached to the touchscreens. Multiple layers can be attached to different columns of the touchscreen with isolated materials between layers. By activating more sensing nodes, we can increase the resolution and range of our applications, which provide us with more possibilities. Another solution to enable more sensing nodes is designing the extension layout in an X-Y matrix configuration as shown in Section 6.3. To minimize the effect between neighboring sensing electrodes, we suggest a gap between attached strips larger than 2*mm* on the touchscreen. We also suggest an isolation gap between layers into which we inserted a 4*mm* isolated rubber in each joint node.

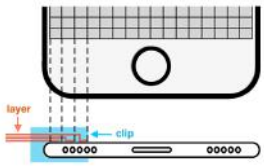

Fig. 13. Possible design for more sensing nodes.

8 CONCLUSION

FlexTouch enables large-scale, passive, and low-cost interaction sensing interfaces by extending the capacitive sensing capability of touchscreens into the ambient environment. It can support a variety of large-scale interaction applications by attaching customized conductive strips to the edge of the touchscreen. We demonstrated that our technique allows for easy fabrication of touch interfaces via a variety of commercially available conductive materials and fabrication approaches. Through a series of evaluation studies, we showed that *FlexTouch* supports long-range touch interaction sensing for up to 4 meters as well as everyday object presence detection for up to 2 meters. Then we demonstrated the versatility and feasibility of *FlexTouch* by implementing and evaluating applications in the domain of body posture recognition, activity detection, object presence detection, and enhanced fitness tracking experiences.

9 ACKNOWLEDGEMENT

We would like to thank all our study participants for their time, effort, and patience. We would like to thank Maggie Chen for the voiceover of the demo video and Matt Andryc for his constructive comments. Our work is supported by the National Key Research and Development Plan of China under Grant No. 2016YFB1001402, the Natural Science Foundation of China under Grant No.: 61521002 and 61572276. Our work is also supported by the Beijing Key Lab of Networked Multimedia.

REFERENCES

[1] Liwei Chan, Stefanie Müller, Anne Roudaut, and Patrick Baudisch. 2012. CapStones and ZebraWidgets: Sensing Stacks of Building Blocks, Dials and Sliders on Capacitive Touch Screens. In *Proceedings of the SIGCHI Conference on Human Factors in Computing Systems (CHI '12)*. ACM, New York, NY, USA, 2189–2192. https://doi.org/10.1145/2207676.2208371

[2] Jerry Alan Fails and Dan Olsen Jr. 2002. Light Widgets: Interacting in Every-day Spaces. In *Proceedings of the 7th International Conference on Intelligent User Interfaces (IUI '02)*. ACM, New York, NY, USA, 63–69. https://doi.org/10.1145/502716.502729

[3] Chuhan Gao, Xinyu Zhang, and Suman Banerjee. 2018. Conductive Inkjet Printed Passive 2D TrackPad for VR Interaction. In *Proceedings of the 24th Annual International Conference on Mobile Computing and Networking, MobiCom 2018, New Delhi, India, October 29 - November 02, 2018*. 83–98. https://doi.org/10.1145/3241539.3241546

[4] Nan-Wei Gong, Jürgen Steimle, Simon Olberding, Steve Hodges, Nicholas Edward Gillian, Yoshihiro Kawahara, and Joseph A. Paradiso. 2014. PrintSense: A Versatile Sensing Technique to Support Multimodal Flexible Surface Interaction. In *Proceedings of the SIGCHI Conference on Human Factors in Computing Systems (CHI '14)*. ACM, New York, NY, USA, 1407–1410. https://doi.org/10.1145/2556288.2557173

[5] Tobias Grosse-Puppendahl, Christian Holz, Gabe Cohn, Raphael Wimmer, Oskar Bechtold, Steve Hodges, Matthew S. Reynolds, and Joshua R. Smith. 2017. Finding Common Ground: A Survey of Capacitive Sensing in Human-Computer Interaction. In *Proceedings of the 2017 CHI Conference on Human Factors in Computing Systems (CHI '17)*. ACM, New York, NY, USA, 3293–3315. https://doi.org/10.1145/3025453.3025808

[6] Anhong Guo, Robert Xiao, and Chris Harrison. 2015. CapAuth: Identifying and Differentiating User Handprints on Commodity Capacitive Touchscreens. *Proceedings of the 2015 International Conference on Interactive Tabletops & Surfaces - ITS '15* (2015), 59–62. https://doi.org/10.1145/2817721.2817722

[7] Chris Harrison and Scott E. Hudson. 2008. Scratch Input: Creating Large, Inexpensive, Unpowered and Mobile Finger Input Surfaces. In *Proceedings of the 21st Annual ACM Symposium on User Interface Software and Technology (UIST '08)*. ACM, New York, NY, USA, 205–208. https://doi.org/10.1145/1449715.1449747

[8] Christian Holz, Senaka Buthpitiya, and Marius Knaust. 2015. Bodyprint: Biometric User Identification on Mobile Devices Using the Capacitive Touchscreen to Scan Body Parts. In *Proceedings of the 33rd Annual ACM Conference on Human Factors in Computing Systems (CHI '15)*. ACM, New York, NY, USA, 3011–3014. https://doi.org/10.1145/2702123.2702518

[9] Kaori Ikematsu and Itiro Siio. 2018. Ohmic-Touch: Extending Touch Interaction by Indirect Touch Through Resistive Objects. In *Proceedings of the 2018 CHI Conference on Human Factors in Computing Systems (CHI '18)*. ACM, New York, NY, USA, Article 521, 8 pages. https://doi.org/10.1145/3173574.3174095

[10] Kunihiro Kato and Homei Miyashita. 2015. Creating a Mobile Head-mounted Display with Proprietary Controllers for Interactive Virtual Reality Content. *Proceedings of the 28th Annual ACM Symposium on User Interface Software & Technology - UIST '15 Adjunct* (2015), 35–36. https://doi.org/10.1145/2815585.2817776

[11] Kunihiro Kato and Homei Miyashita. 2015. ExtensionSticker: A Proposal for a Striped Pattern Sticker to Extend Touch Interfaces and Its Assessment. In *Proceedings of the 33rd Annual ACM Conference on Human Factors in Computing Systems (CHI '15)*. ACM, New York, NY, USA, 1851–1854. https://doi.org/10.1145/2702123.2702500

[12] Kunihiro Kato and Homei Miyashita. 2016. 3D Printed Physical Interfaces That Can Extend Touch Devices. In *Proceedings of the 29th Annual Symposium on User Interface Software and Technology (UIST '16 Adjunct)*. ACM, New York, NY, USA, 47–49. https://doi.org/10.1145/2984751.2985700

[13] Yoshihiro Kawahara, Steve Hodges, Benjamin S. Cook, Cheng Zhang, and Gregory D. Abowd. 2013. Instant Inkjet Circuits: Lab-based Inkjet Printing to Support Rapid Prototyping of UbiComp Devices. In *Proceedings of the 2013 ACM International Joint Conference on Pervasive and Ubiquitous Computing (UbiComp '13)*. ACM, New York, NY, USA, 363–372. https://doi.org/10.1145/2493432.2493486

[14] Huy Viet Le, Thomas Kosch, Patrick Bader, Sven Mayer, and Niels Henze. 2018. PalmTouch: Using the Palm As an Additional Input Modality on Commodity Smartphones. In *Proceedings of the 2018 CHI Conference on Human Factors in Computing Systems (CHI '18)*. ACM, New York, NY, USA, Article 360, 13 pages. https://doi.org/10.1145/3173574.3173934

[15] Simon Olberding, Nan-Wei Gong, John Tiab, Joseph A. Paradiso, and Jürgen Steimle. 2013. A Cuttable Multi-touch Sensor. In *Proceedings of the 26th Annual ACM Symposium on User Interface Software and Technology (UIST '13)*. ACM, New York, NY, USA, 245–254. https:

//doi.org/10.1145/2501988.2502048

[16] Simon Olberding, Sergio Soto Ortega, Klaus Hildebrandt, and Jürgen Steimle. 2015. Foldio: Digital Fabrication of Interactive and Shape-Changing Objects With Foldable Printed Electronics. In *Proceedings of the 28th Annual ACM Symposium on User Interface Software and Technology (UIST '15)*. ACM, New York, NY, USA, 223–232. https://doi.org/10.1145/2807442.2807494

[17] Simon Olberding, Michael Wessely, and Jürgen Steimle. 2014. PrintScreen: Fabricating Highly Customizable Thin-film Touch-displays. In *Proceedings of the 27th Annual ACM Symposium on User Interface Software and Technology (UIST '14)*. ACM, New York, NY, USA, 281–290. https://doi.org/10.1145/2642918.2647413

[18] Makoto Ono, Buntarou Shizuki, and Jiro Tanaka. 2013. Touch and Activate: Adding Interactivity to Existing Objects Using Active Acoustic Sensing. In *Proceedings of the 26th Annual ACM Symposium on User Interface Software and Technology (UIST '13)*. ACM, New York, NY, USA, 31–40. https://doi.org/10.1145/2501988.2501989

[19] Makoto Ono, Buntarou Shizuki, and Jiro Tanaka. 2014. A Rapid Prototyping Toolkit for Touch Sensitive Objects Using Active Acoustic Sensing. In *Proceedings of the Adjunct Publication of the 27th Annual ACM Symposium on User Interface Software and Technology (UIST'14 Adjunct)*. ACM, New York, NY, USA, 35–36. https://doi.org/10.1145/2658779.2659101

[20] Joseph A. Paradiso, Che King Leo, Nisha Checka, and Kaijen Hsiao. 2002. Passive Acoustic Knock Tracking for Interactive Windows. In *CHI '02 Extended Abstracts on Human Factors in Computing Systems (CHI EA '02)*. ACM, New York, NY, USA, 732–733. https://doi.org/10.1145/506443.506570

[21] Claudio Pinhanez. 2001. The Everywhere Displays Projector: A Device to Create Ubiquitous Graphical Interfaces. In *Ubicomp 2001: Ubiquitous Computing*, Gregory D. Abowd, Barry Brumitt, and Steven Shafer (Eds.). Springer Berlin Heidelberg, Berlin, Heidelberg, 315–331. https://doi.org/10.1007/3-540-45427-6_27

[22] Jun Rekimoto. 2002. SmartSkin: An Infrastructure for Freehand Manipulation on Interactive Surfaces. In *Proceedings of the SIGCHI Conference on Human Factors in Computing Systems (CHI '02)*. ACM, New York, NY, USA, 113–120. https://doi.org/10.1145/503376.503397

[23] Munehiko Sato, Ivan Poupyrev, and Chris Harrison. 2012. Touché: Enhancing Touch Interaction on Humans, Screens, Liquids, and Everyday Objects. In *Proceedings of the SIGCHI Conference on Human Factors in Computing Systems (CHI '12)*. ACM, New York, NY, USA, 483–492. https://doi.org/10.1145/2207676.2207743

[24] Valkyrie Savage, Xiaohan Zhang, and Björn Hartmann. 2012. Midas: Fabricating Custom Capacitive Touch Sensors to Prototype Interactive Objects. In *Proceedings of the 25th Annual ACM Symposium on User Interface Software and Technology (UIST '12)*. ACM, New York, NY, USA, 579–588. https://doi.org/10.1145/2380116.2380189

[25] Martin Schmitz, Martin Herbers, Niloofar Dezfuli, Sebastian Günther, and Max Mühlhäuser. 2018. Off-Line Sensing: Memorizing Interactions in Passive 3D-Printed Objects. In *Proceedings of the 2018 CHI Conference on Human Factors in Computing Systems (CHI '18)*. ACM, New York, NY, USA, Article 182, 8 pages. https://doi.org/10.1145/3173574.3173756

[26] Martin Schmitz, Urgen Steimle, Jochen Huber, Niloofar Dezfuli, and Max Uhlhäuser. 2017. Flexibles: Deformation-Aware 3D-Printed Tangibles for Capacitive Touchscreens. *CHI '17 Proceedings of the 2017 CHI Conference on Human Factors in Computing Systems* (2017), 1001–1014. https://doi.org/10.1145/3025453.3025663

[27] Alien Technology. 2018. ITO manufacture. http://www.h-nxc.com/.

[28] Nirzaree Vadgama and Jürgen Steimle. 2017. Flexy: Shape-Customizable, Single-Layer, Inkjet Printable Patterns for 1D and 2D Flex Sensing. In *Proceedings of the Eleventh International Conference on Tangible, Embedded, and Embodied Interaction (TEI '17)*. ACM, New York, NY, USA, 153–162. https://doi.org/10.1145/3024969.3024989

[29] Andrew D. Wilson and Hrvoje Benko. 2010. Combining Multiple Depth Cameras and Projectors for Interactions on, Above and Between Surfaces. In *Proceedings of the 23Nd Annual ACM Symposium on User Interface Software and Technology (UIST '10)*. ACM, New York, NY, USA, 273–282. https://doi.org/10.1145/1866029.1866073

[30] Robert Xiao, Chris Harrison, and Scott E. Hudson. 2013. WorldKit: Rapid and Easy Creation of Ad-hoc Interactive Applications on Everyday Surfaces. In *Proceedings of the SIGCHI Conference on Human Factors in Computing Systems (CHI '13)*. ACM, New York, NY, USA, 879–888. https://doi.org/10.1145/2470654.2466113

[31] Neng-Hao Yu, Sung-Sheng Tsai, I-Chun Hsiao, Dian-Je Tsai, Meng-Han Lee, Mike Y. Chen, and Yi-Ping Hung. 2011. Clip-on Gadgets: Expanding Multi-touch Interaction Area with Unpowered Tactile Controls. In *Proceedings of the 24th Annual ACM Symposium on User Interface Software and Technology (UIST '11)*. ACM, New York, NY, USA, 367–372. https://doi.org/10.1145/2047196.2047243

[32] Yang Zhang and Chris Harrison. 2018. Pulp Nonfiction: Low-Cost Touch Tracking for Paper. In *Proceedings of the 2018 CHI Conference on Human Factors in Computing Systems (CHI '18)*. ACM, New York, NY, USA, Article 117, 11 pages. https://doi.org/10.1145/3173574.3173691

[33] Yang Zhang, Gierad Laput, and Chris Harrison. 2017. Electrick: Low-Cost Touch Sensing Using Electric Field Tomography. In *Proceedings of the 2017 CHI Conference on Human Factors in Computing Systems (CHI '17)*. ACM, New York, NY, USA, 1–14. https://doi.org/10.1145/3025453.3025842

[34] Yang Zhang, Chouchang (Jack) Yang, Scott E. Hudson, Chris Harrison, and Alanson Sample. 2018. Wall++: Room-Scale Interactive and Context-Aware Sensing. In *Proceedings of the 2018 CHI Conference on Human Factors in Computing Systems (CHI '18)*. ACM, New York, NY, USA, Article 273, 15 pages. https://doi.org/10.1145/3173574.3173847